[redacted]L

Copy No. 43
RM No. SL9D21

RESEARCH MEMORANDUM

for the

Air Materiel Command, U. S. Air Force

PRELIMINARY RESULTS OF A FREE-FLIGHT INVESTIGATION OF THE STATIC STABILITY AND AILERON CONTROL CHARACTERISTICS OF $\frac{1}{6}$-SCALE MODELS OF THE BELL MX-776

By

David H. Michal and Grady L. Mitcham

Langley Aeronautical Laboratory
Langley Air Force Base, Va.

CLASSIFIED DOCUMENT

CLASSIFICATION CHANGED
To UNCLASSIFIED
By authority of NACA Research Abstract No. 116 dated 7-9-57

CLASSIFICATION CHANGED
To UNCLASSIFIED
By authority of RE 1345 dated 4-17-58

NATIONAL ADVISORY COMMITTEE
FOR AERONAUTICS

WASHINGTON

JUL 1949

[redacted]AL

NACA RM No. SL9D21

[redacted]

NATIONAL ADVISORY COMMITTEE FOR AERONAUTICS

RESEARCH MEMORANDUM

for the

Air Materiel Command, U. S. Air Force

PRELIMINARY RESULTS OF A FREE-FLIGHT INVESTIGATION OF THE STATIC STABILITY AND AILERON CONTROL CHARACTERISTICS OF $\frac{1}{6}$-SCALE MODELS OF THE BELL MX-776

By David H. Michal and Grady L. Mitcham

SUMMARY

An investigation of the static longitudinal stability, static directional stability, and aileron control characteristics at transonic and supersonic speeds is being made of $\frac{1}{6}$-scale rocket-propelled models of the Bell MX-776. A stability investigation has been made of two symmetrical models with controls undeflected and centers of gravity one-half and one-body diameter, respectively, ahead of the equivalent design center-of-gravity location of the full-scale version. Both models developed large normal-force coefficients in both the subsonic and supersonic ranges which indicated longitudinal instability at low angles of attack. The side-force coefficients were small for both models and indicated that the models were directionally stable. A possible tendency toward dynamic directional instability in the transonic region was indicated by short-period oscillations of the side forces.

The results showed a partial-span inboard aileron to be ineffective or to cause negative control in the transonic region when deflected approximately 5° but not when deflected 10°. An investigation of drag showed it to increase with a rearward movement of the center of gravity. This indicates an increase in the trim angle of attack as could be caused by a decrease in static stability.

INTRODUCTION

At the request of the Air Materiel Command, Army Air Forces, the Langley Pilotless Aircraft Research Division is conducting tests

[redacted]

of $\frac{1}{6}$-scale models of the Bell MX-776 at the NACA Pilotless Aircraft Research Station, Wallops Island, Va. The purpose of these tests is to investigate the static longitudinal stability, static directional stability, and aileron control characteristics of the MX-776. This paper covers the flights of six models which were launched during a 3-month period that ended in September 1948. Models 1 and 2 were instrumented to measure normal and transverse acceleration and were flown with 0° deflection of the control surfaces. Models 3, 4, 5, and 6 were instrumented to measure rolling velocity and were flown with ailerons deflected 0°, 4.7°, 10.0°, and 4.6°, respectively.

Some drag data were obtained from all but one flight. The tests were conducted by means of free-flight techniques described in references 1 and 2.

SYMBOLS

M	Mach number
R	Reynolds number based on a body diameter (0.473 ft)
$\frac{pb}{2V}$	tip helix angle, radians
p	rolling velocity, radians per second
b	diameter of circle swept by wing tips (2.072 ft)
V	flight-path velocity, feet per second
q	dynamic pressure, pounds/square foot $\left(\frac{\rho V^2}{2}\right)$
ρ	density, slugs/cubic foot
S_F	body frontal area (0.1758 sq ft)
C_N	normal-force coefficient $\left(\frac{\text{Normal-force}}{qS_F}\right)$
C_Y	side-force coefficient $\left(\frac{\text{Side force}}{qS_F}\right)$
C_D	drag coefficient $\left(\frac{\text{Drag}}{qS_F}\right)$
δ_a	average aileron deflection measured in the free-stream direction, degrees
W	weight of model, pounds

a_n normal acceleration, feet per second per second

a_y transverse acceleration, feet per second per second

g acceleration due to gravity, feet per second per second

MODELS AND TESTS

Models

The $\frac{1}{6}$-scale models used for this investigation were supplied by the MX-776 contractor. The fuselages were constructed of balsa wood with aluminum castings to serve as mounts for the metal wings and tails. The nose sections were made of plexiglas and contained a small radio transmitter.

Figure 1 shows a three-view drawing of the model. The pertinent general specifications are given in table I, and the model characteristics are given in table II. The areas given in figure 1 include wing areas obtained by extending all leading and trailing edges to body center line. The center of gravity shown in figure 1 is the corresponding full-scale-design location. For the models covered by the present paper the centers of gravity were located forward of this point as indicated in table II. Photographs of one of the models are shown in figures 2 to 4.

The models were propelled by a two-stage rocket-propulsion system to a Mach number of about 1.7. The booster delivered 3100 pounds of thrust for 1.5 seconds, and the sustainer motor developed 2000 pounds of thrust for 0.9 second.

Tests

The models were launched from a rail-type launcher (fig. 3) set at an elevation angle of approximately 60°. The flight-path velocity was generally obtained with a continuous-wave Doppler velocimeter radar unit. For the lower speed ranges of some of the models, the velocity was calculated using drag data measured for the other models. Atmospheric data were obtained by the use of radiosondes. Models 1 and 2 were equipped with two-channel nose-type telemeters that transmitted continuous signals of normal and transverse acceleration to two ground stations. These stations recorded the signals in the form of time histories. The accelerations were measured relative to the center line of the models. Time histories of the rolling velocity were obtained with spinsonde radio equipment for the four aileron-effectiveness models. A plot of Reynolds number against Mach number, shown in figure 5, indicates the scale of the tests.

[redacted]

REDUCTION OF DATA

Mach number was determined by use of radiosonde data and Doppler flight-path velocity. The values of normal and transverse accelerations obtained from the telemeter time histories for the deceleration phase of the flights were converted to coefficients by the relationships

$$C_N = \frac{Wa_n}{qS_{Fg}}$$

and

$$C_Y = \frac{Wa_y}{qS_{Fg}}$$

The rates of roll from the spinsonde time histories were used to obtain tip helix angles as functions of Mach number. The values of drag were obtained by the graphic differentiation of the curve of Doppler flight-path velocity against time.

ACCURACY

The accuracy of the tests is estimated to be within the following limits:

C_N	±0.065
C_Y	±0.032
$\frac{pb}{2V}$	±0.001
C_D	±0.02
M	±0.01

The calculated flight-path velocities and corresponding Mach numbers are estimated to be accurate to ±5 percent.

RESULTS AND DISCUSSION

Stability

The data obtained from the flight of model 1 are shown in figure 6 as variation of normal-force and side-force coefficients with Mach number. Although the center of gravity of this model was one-half body diameter

[redacted]

ahead of the design location and all controls were neutral, the model developed large normal forces which at some speeds exceeded the limit of the measuring instrument. The actual normal-force coefficients could be determined only for the Mach number ranges from 0.76 to 0.95 and 1.65 to 1.69. Inasmuch as the normal acceleration exceeded the limits of the instrumentation in the Mach number range from 0.95 to 1.65, no values for C_N were obtained in this range, but the maximum value of normal acceleration for the instrumentation was used to indicate the minimum possible C_N as shown by the dash part of the curve in figure 6. Model 2 was similar to model 1 with the exception of the center-of-gravity location which was approximately one body diameter ahead of the design center of gravity. The data for model 2 are presented in figure 7. The values of C_N were smaller for model 2 than for model 1 for corresponding Mach numbers which indicated that model 2 was trimming at smaller angles of attack. For model 2 the change in sign of C_N at a Mach number of approximately 0.925 indicates that the model was disturbed and changed from a trim point at a positive angle of attack to one at a negative angle of attack. No force data were obtained in the Mach number range from 0.95 to 0.97 and is so indicated in figure 7 by dash lines. Unpublished supersonic wind-tunnel data showed a model with the center of gravity at the design location to be unstable at angles of attack near 0°, with trim points at approximately ±6° at a Mach number of 1.28 and ±4° at a Mach number of 1.72. The values of C_Y (figs. 6 and 7) were sufficiently small throughout the speed range of the tests to indicate static directional stability. The fact that short-period oscillation of the side forces occurred as the models decelerated through the transonic region indicates possible tendency towards dynamic directional instability in this region.

Aileron Effectiveness

The results of the data obtained from the flights of models 3, 4, 5, and 6 are shown in figure 8 as plots of $pb/2V$ against Mach number. Doppler flight-path velocity was obtained for a Mach number range from 1.26 to 1.48 for model 3, from 0.95 to 1.73 for model 4, and from 1.18 to 1.78 for model 5. Doppler flight-path velocity was not obtained for model 6. Tip helix angles were derived for each model by using these velocities and the rolling velocities obtained from the spinsonde records. These curves of $pb/2V$ were extended by using calculated flight-path velocities in conjunction with the measured rolling velocities. The results from the test of a partial-span inboard aileron deflected 4.7° (model 4) showed that the rolling effectiveness decreased abruptly in the Mach number range from 0.85 to 0.95. The direction of roll was reversed in the Mach number range between 0.93 and 1.07 and showed a gradual increase in aileron rolling effectiveness up to a Mach number of 1.40. The results of the test of the same aileron configuration deflected 4.6° (model 6) showed the same general characteristics except in the Mach number range from 0.93 to 1.07. In this Mach number range model 6 showed an almost complete loss of aileron control but no actual control reversal. The results of the same aileron configuration deflected 10.0° (model 5) showed no reversal, but showed an abrupt decrease in rolling

effectiveness in the Mach number range from 0.85 to 0.90 and a gradual decrease in rolling effectiveness up to the maximum Mach number tested of 1.78.

Drag

The exact drag of the configuration cannot be evaluated because of the erratic flight caused by the instability of the models. The approximate drag data presented in figure 9 as variation of drag coefficients with Mach number show the more stable models (models 2 and 3) to have had less drag than the others and therefore must have been trimming at smaller angles of attack.

CONCLUDING REMARKS

The present MX-776 has a region of static longitudinal instability near 0° angle of attack. This region appears to be largest in the transonic range and to decrease with an increase in Mach number in the supersonic range. The configuration appeared to be statically stable directionally with the possibility of a tendency toward dynamic directional instability in the transonic range. Additional tests are planned for models modified to improve the stability.

Langley Aeronautical Laboratory
National Advisory Committee for Aeronautics
Langley Air Force Base, Va.

David H. Michal
David H. Michal
Aeronautical Research Scientist

Grady L. Mitcham
Grady L. Mitcham
Aeronautical Engineer

Approved:

Robert R. Gilruth
Chief of Pilotless Aircraft Research Division

GMF

[redacted]

REFERENCES

1. Sandahl, Carl A. and Marino, Alfred A.: Free-Flight Investigation of Control Effectiveness of Full-Span 0.2-Chord Plain Ailerons at High Subsonic, Transonic, and Supersonic Speeds to Determine Some Effects of Section Thickness and Wing Sweepback. NACA RM No. L7D02, 1947.

2. Alexander, Sidney R.: Flight Investigation to Determine the Aerodynamic Characteristics of Rocket-Powered Models Representative of a Fighter-Type Airplane Configuration Incorporating an Inverse-Taper Wing and a Vee Tail. NACA RM No. L8G29, 1948.

[redacted]

TABLE I

GENERAL SPECIFICATIONS

[Fuselage: Over-all length, 68.637 in.; maximum diameter, 5.678 in.]

	Aft horizontal wings	Forward horizontal wings	Aft vertical fins	Forward vertical fins
Aspect ratio	3.02	3.16	2.00	3.73
Total span, in.	24.866	18.917	15.166	10.48
Total area, sq ft	1.422	.788	.796	.204
Angle of incidence, deg	0	0	0	0
Dihedral, deg	0	0	0	0
Sweep, 0.5 chord, deg	10.6	10.6	10.5	10.3
Airfoil section	Symmetrical wedge of 0.05 thickness ratio			

NACA

TABLE II

MODEL CHARACTERISTICS DURING THE UNPOWERED PORTION OF THE FLIGHT

[Station numbers correspond to distance in in. from point of nose]

Models	Instrumentation	Aileron deflection (deg)	Weight (lb)	C.G. location station
1	Telemeter	0	46.6	35.7
2	Telemeter	0	54.0	32.9
3	Spinsonde	0	48.0	33.9
4	Spinsonde	4.7	43.2	35.7
5	Spinsonde	10.0	43.5	35.6
6	Spinsonde	4.6	44.3	35.9

[redacted]

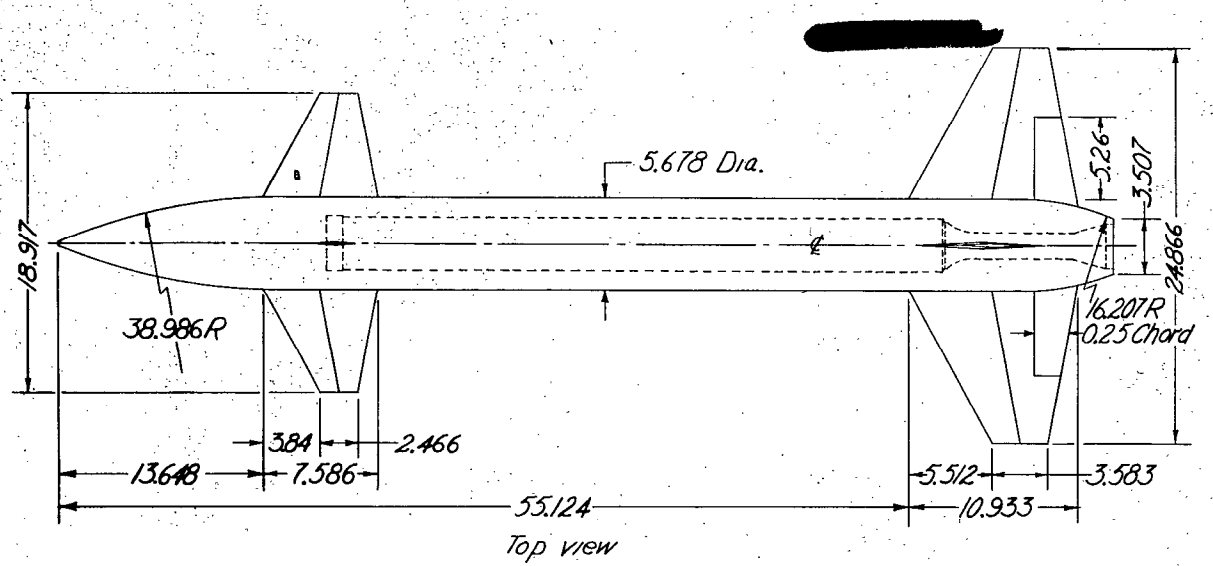

	Included area	Aspect ratio
Aft hor. wing	1.422 ft.²	3.02
Aft vert. fin	0.796 ft.²	2.00
Forward hor. wing	0.788 ft.²	3.16
Forward vert. fin	0.204 ft.²	3.73

All airfoils are of a symmetrical wedge section of 0.05 thickness ratio

All dimensions are in inches

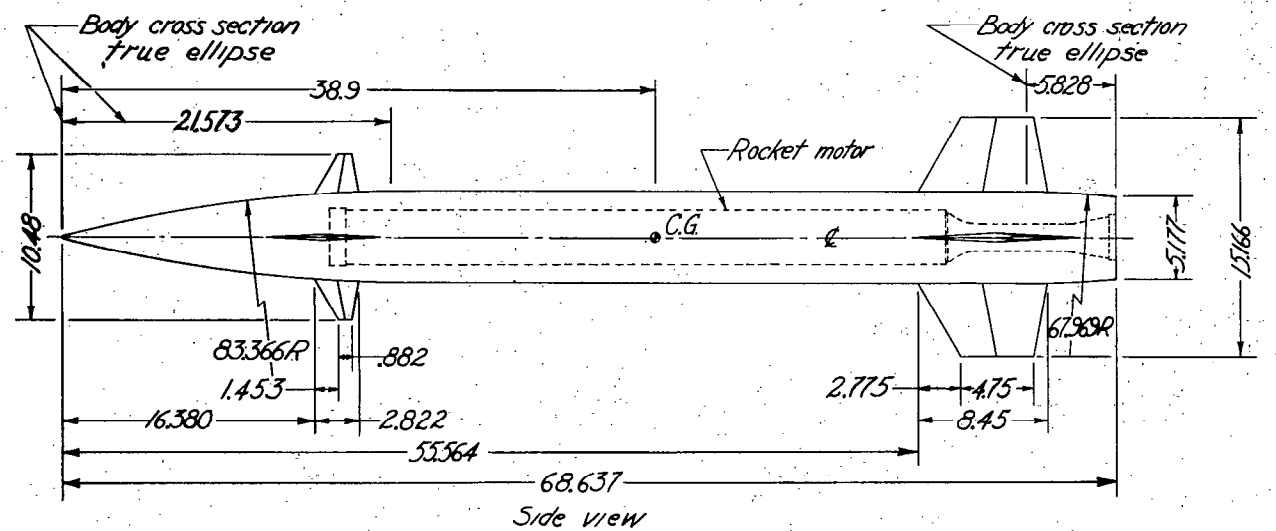

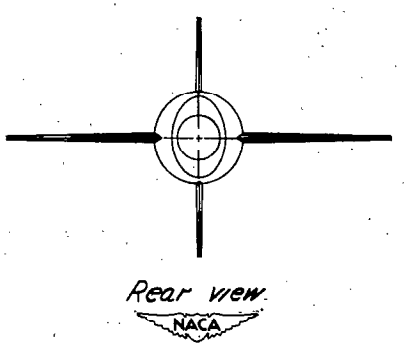

Figure 1.- General arrangement of $\frac{1}{6}$-scale MX-776 rocket-powered flight-test model.

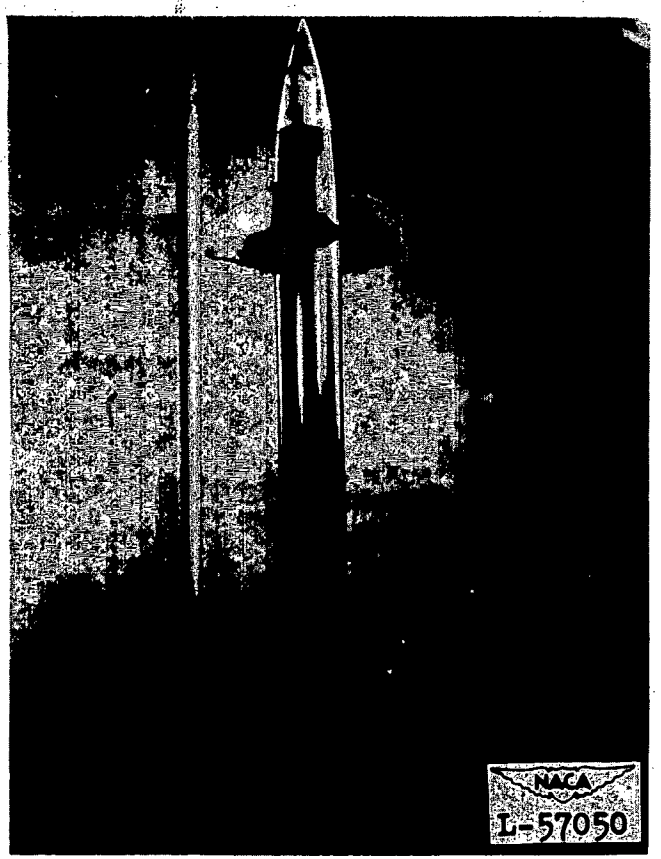

Figure 2.- MX-776 rocket-powered flight-test model.

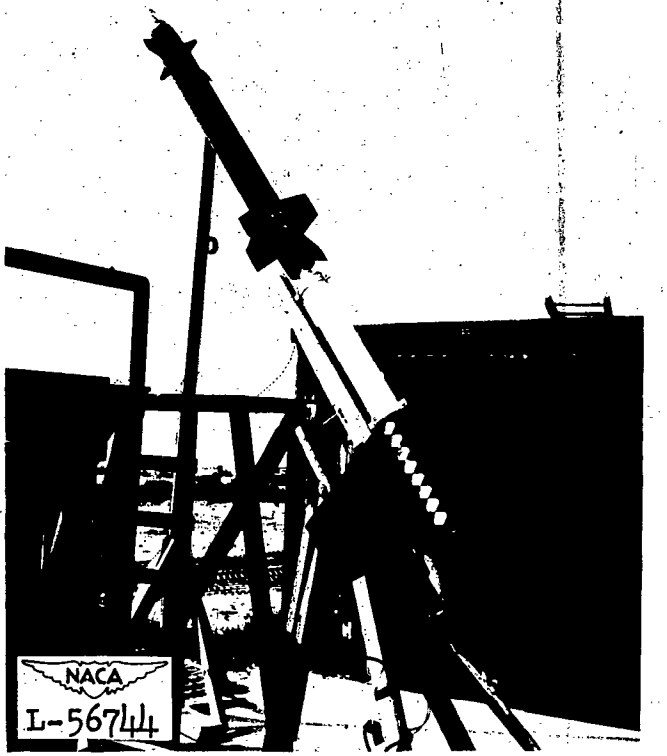

Figure 3.- Model and booster on launcher.

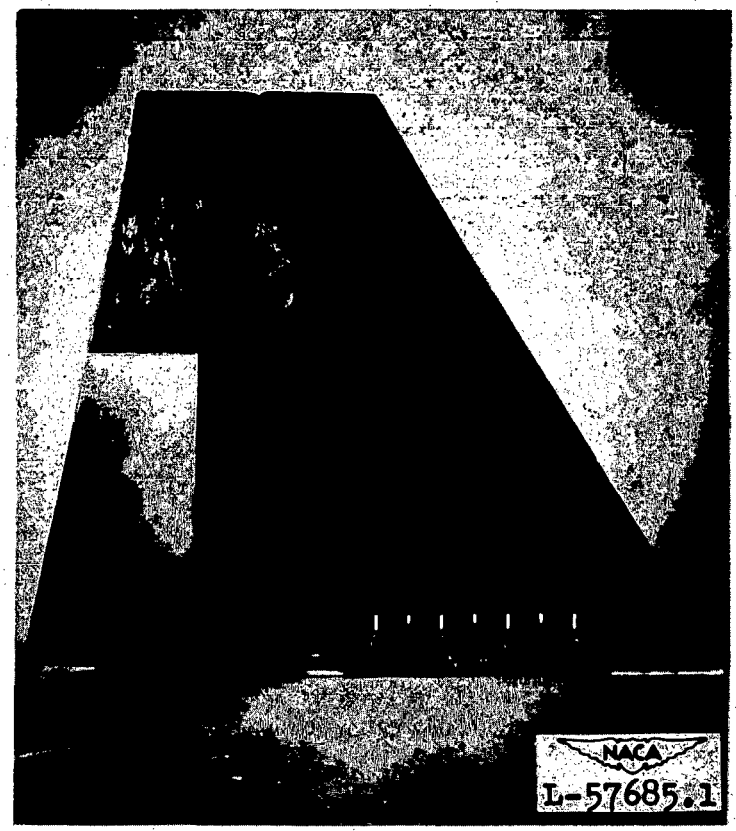

Figure 4.– Aft horizontal wing with partial–span inboard aileron.

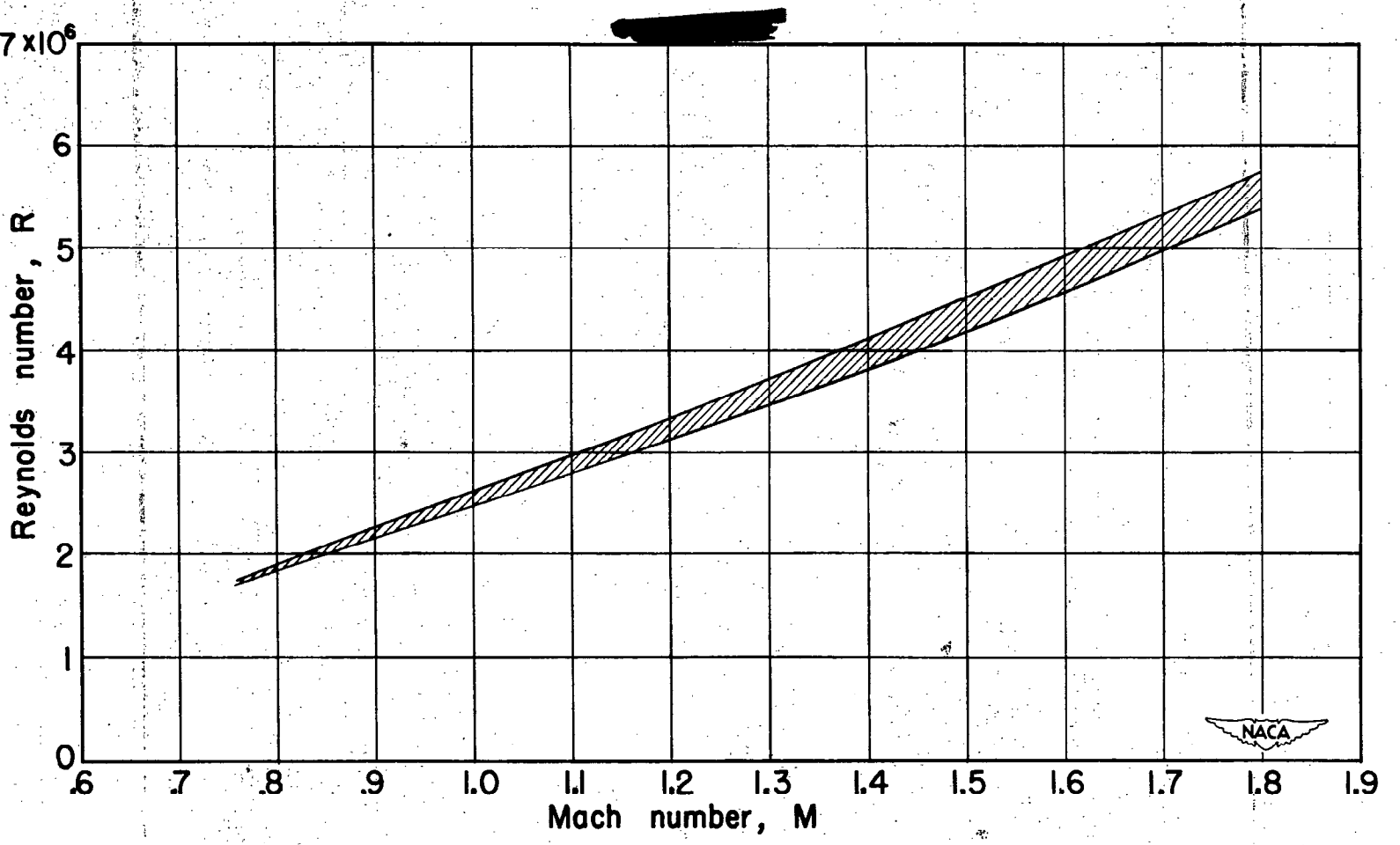

Figure 5.- Variation of Reynolds number with Mach number for the range of climatic conditions encountered during the tests.

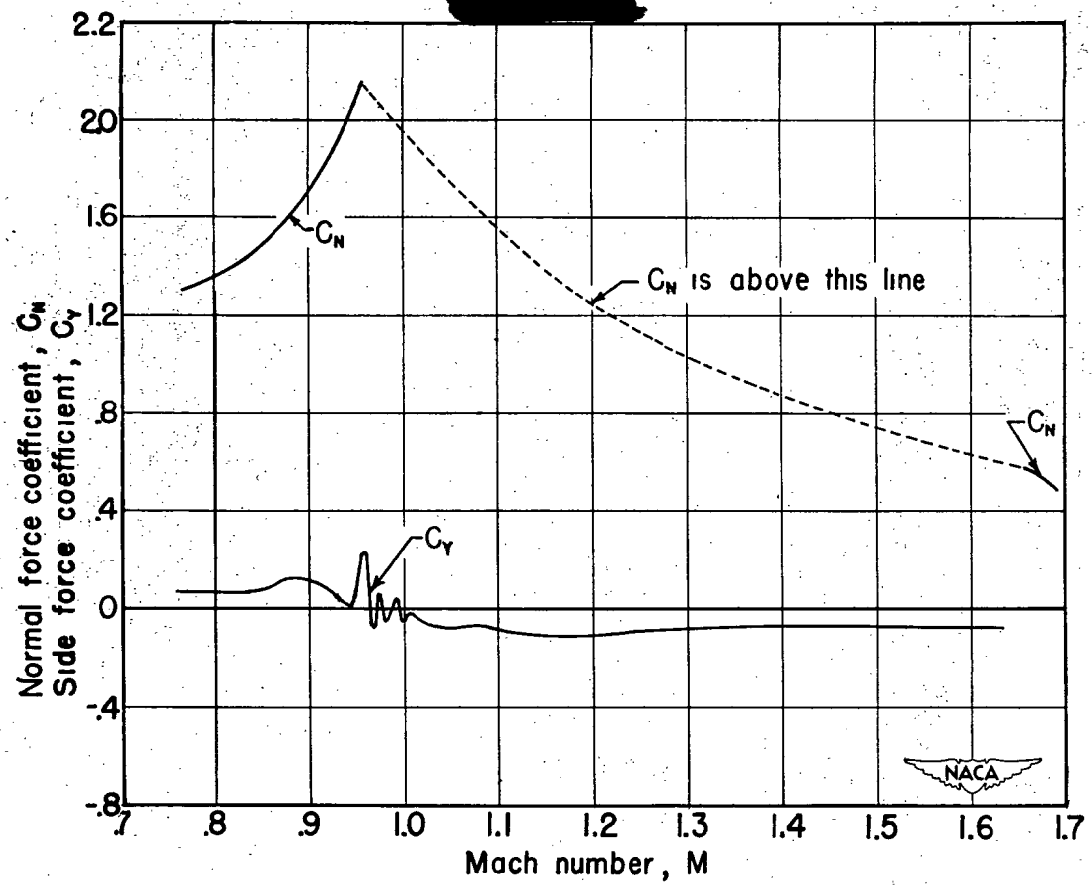

Figure 6.– Variation of normal–force coefficient and side force coefficient with Mach number; c.g. at station 35.7; $\delta_a = 0^\circ$; model 1.

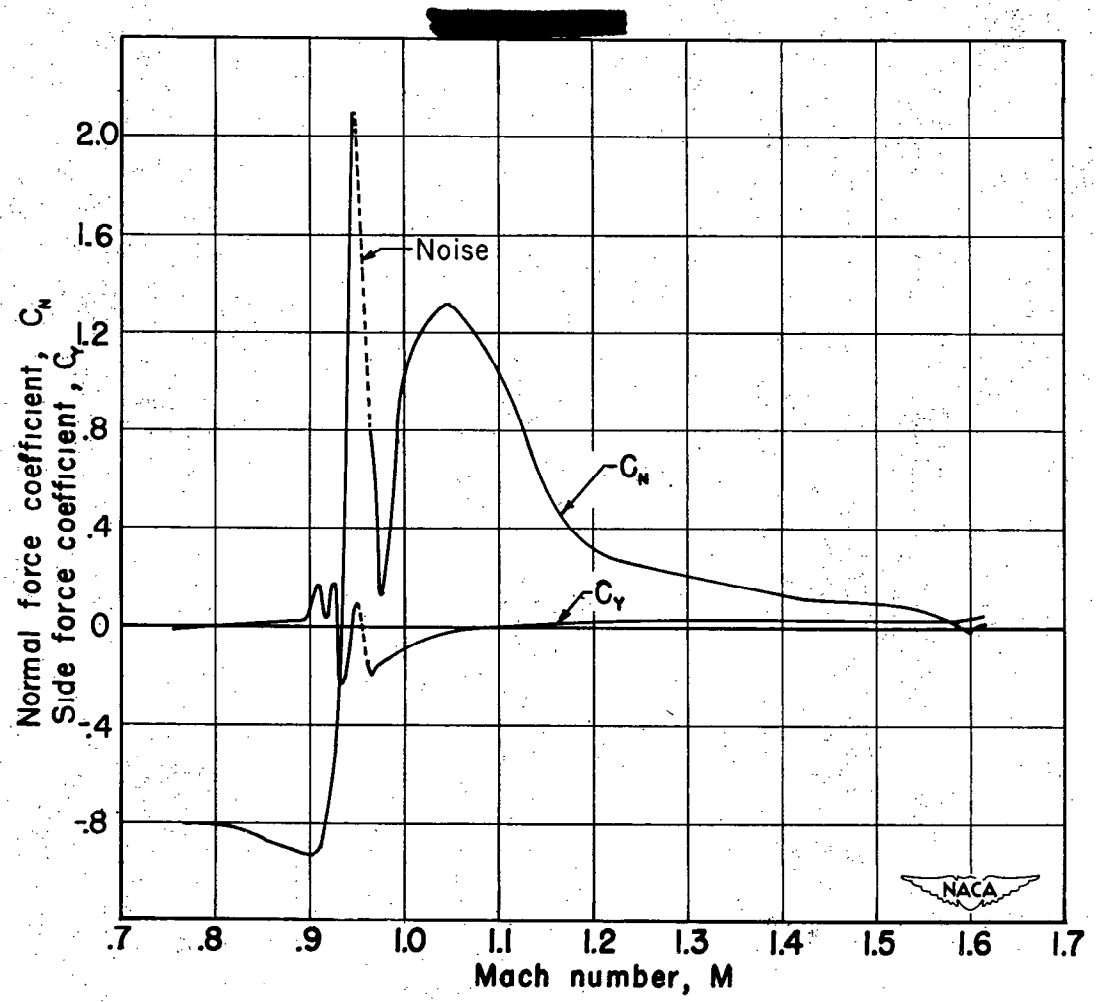

Figure 7.— Variation of normal-force coefficient and side-force coefficient with Mach number; c.g. at station 32.9; $\delta_a = 0^\circ$; model 2.

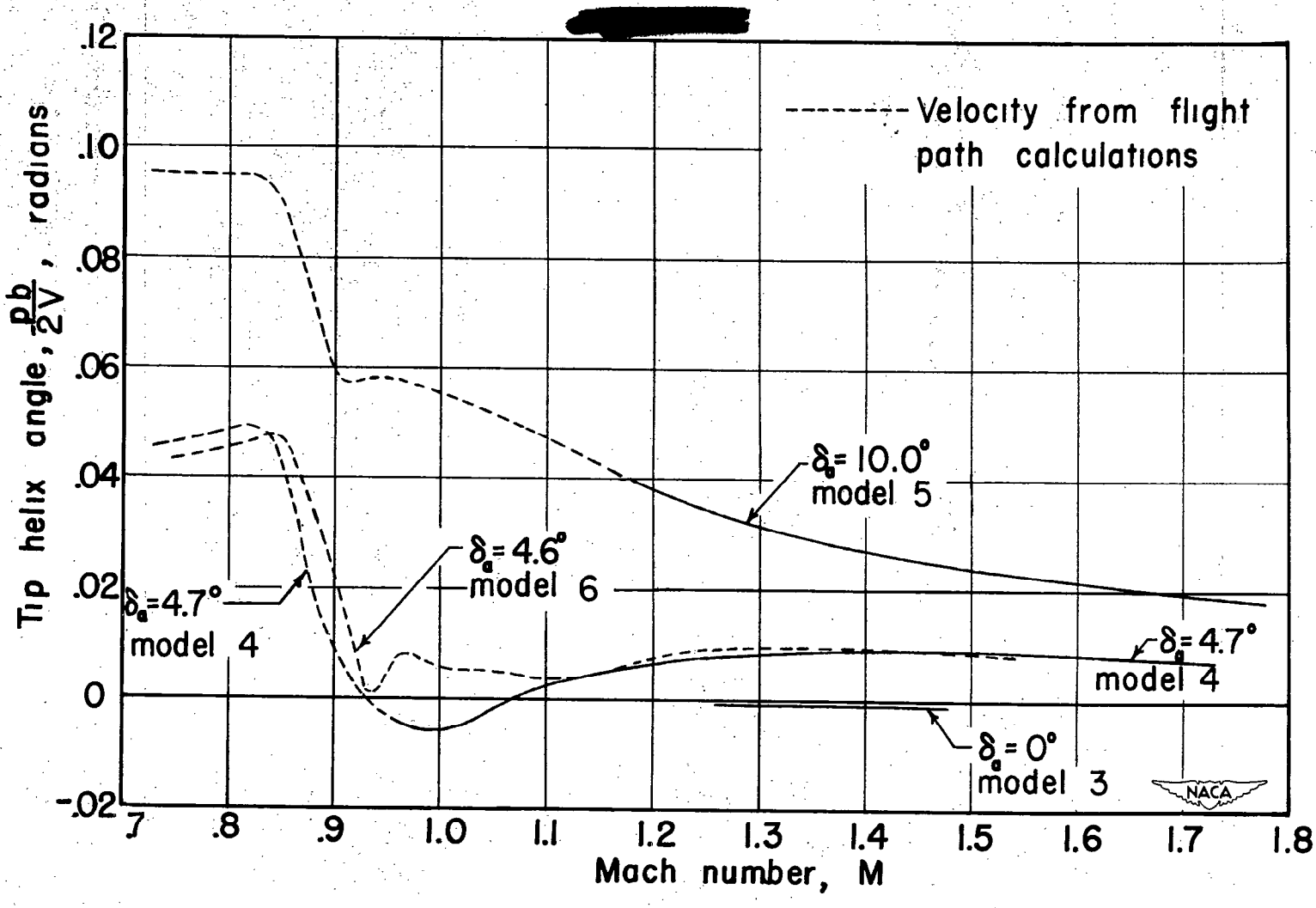

Figure 8.– Variation of tip helix angle with Mach number.

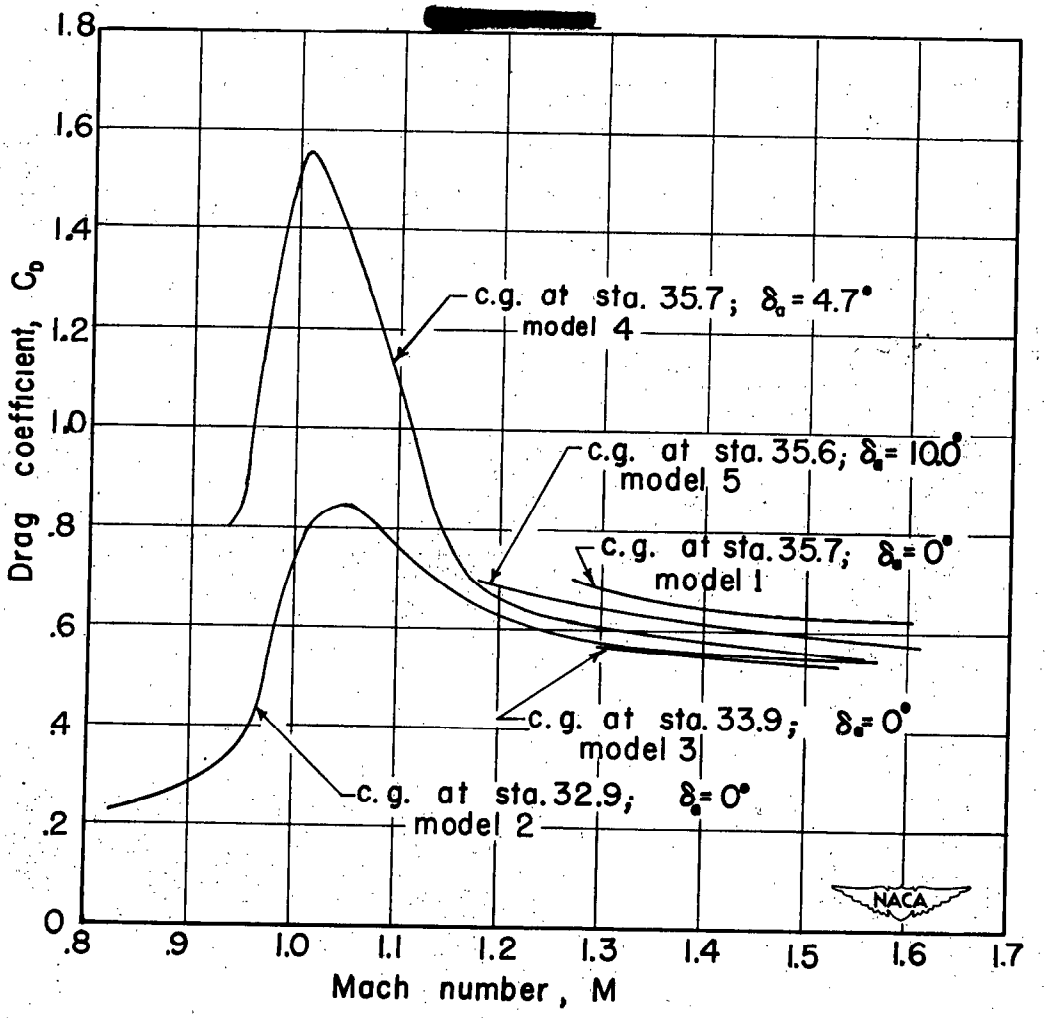

Figure 9.– Variation of trim drag coefficients with Mach number.